Study of Salt Neutrino Detector

Masami Chiba, Toshio Kamijo*, Miho Kawaki, Athar Husain,
Masahide Inuzuka, Maho Ikeda, Osamu Yasuda

Department of Physics, Tokyo Metropolitan University
1-1 Minami-Ohsawa Hachioji-shi, Tokyo, 192-0397, Japan
**Department of Electrical Engineering, Tokyo Metropolitan University*
1-1 Minami-Ohsawa Hachioji-shi, Tokyo, 192-0397, Japan

Abstract. Rock salt is studied as a radio wave transmission medium in an ultra high energy (UHE) cosmic neutrino detector. The radio wave would be generated by Askar'yan effect (coherent Chrenkov radiation from negative excess charges in the electromagnetic shower) in the UHE neutrino interaction in the rock salt. We collected the samples of the rock salts from various rock salt mines in order to investigate whether they have a possibility as a Salt Neutrino Detector (SND) sites or not. As a tentative result, the absorption length of the rock salt samples was measured to be between 40m and 400m at 1 GHz

INTRODUCTION

Several cosmologically distant astrophysical systems could produce ultra-high-energy (UHE) cosmic neutrinos [1] over the energy of 10^{15} eV or PeV whose flux probably exceeds that of the atmospheric neutrino [2]. Therefore, in spite of the very low flux, we could detect extraterrestrial neutrinos coming from far distance over 100Mpc (10 million light years) without the atmospheric neutrino background. UHE neutrinos are produced by astrophysical sources in cosmological distance such as Quasars (QSOs) or Active Galactic Nuclei (AGNs) and Gamma Ray Bursts (GRBs). They follow the production and decay of related unstable hadrons: pions, kaons, and charmed mesons. These unstable hadrons could be produced when the accelerated protons interact with the ambient photon or protons present in the environment. The electron and muon neutrinos are mainly produced in the decay chain of charged pions whereas the tau neutrinos are mainly produced in the decay chain of charmed mesons in the same collisions at a suppressed level.

The maximum energy of observed cosmic rays (protons or nuclei) exceeds 10^{20} eV [3]. The energy is over the allowed energy for cosmic rays traveled from the extra galaxy over 50 Mpc, which loses its energy in scattering processes against 3° K cosmic background radiations. (GZK cutoff) [4]. It is one of the centers of attention in astrophysics and high-energy physics [5]. On the other hand, a neutrino scarcely interacts with the 3° K cosmic background radiation, and then it can travel long distance without losing the energy. The aim of the UHE-neutrino detection is to study, (1) the UHE neutrino interaction, which is not afforded by an artificial neutrino beam, generated by an accelerator, (2) the neutrino mass problem through neutrino oscillation effect after the long flight distance, (3) the UHE accelerating mechanism of the proton existing in the universe.

In order to detect the UHE neutrinos, we need a huge mass (at least 10^9 tons) of the detector since neutrinos interact in the detector volume via weak interactions and the flux of UHE neutrinos is very low. However, from the practical point of view, it is difficult to construct such a huge detector. Therefore we decide to use the rock salt mine in nature as the UHE neutrino detector, Salt Neutrino Detector (SND). For such a huge detector we could not give any treatment on it e.g. purification of the medium etc., then we should use it as it is naturally existed.

The interaction cross-section of UHE neutrino increases up to 10^{-33} cm^2 but still it is not so large compared with the other interactions [6]. Due to the increase, the number of upward neutrinos is suppressed due to the absorption by the earth. The differential shadow factor by the earth and the neutrino fluxes are presented in ref. [6]. A moderate event rate over PeV neutrinos is expected to be 10/year by 1km $\times$ 1km $\times$ 1km of 2×10^9 tons of rock salt from QSOs or AGNs and GRBs by Athar, H. [7].

The mass of the detector required to measure the UHE neutrinos should be compared with the existing large neutrino detector, Super Kamiokande (S-K), which consists of 5×10^4 tons of pure water [8]. SND is 4×10^4 times large compared with S-K. They detect visible light generated by Cherenkov effect in the pure water. The transparency (absorption length) in pure water is 100 m at most. On the contrary, rock salt is one of the most transparent materials for radio wave. The transparency of electromagnetic wave in microwave region or longer wavelength is expected to be larger than that of the optical wavelength in pure water. Therefore moderate number of radio wave sensors could detect the neutrino interaction in the massive rock salt.

Coherent Cherenkov radiation

Almost one third of the energy in the hadronic shower generated at UHE neutrino interaction is given to the electromagnetic part by two-photon decays of neutral pions. Askar'yan, G. A. proposed detection of radio emission with coherent amplification from the excess negative charges of an electron-photon shower in a dense material [9]. In the range of wavelengths greater than the dimensions of the excess electron cluster, the intensity of the radiation is proportional to the square of the total excess electron track length. The density of the medium determines the dimensions of the localized region of shower particles. The shower size and the wavelength determine how much the radiation is in coherence. The small attenuation of the radio waves in rock salt, marble, granite, and etc. underground is preferable. Also the absorption of radio waves in the ground of the moon should be small to use such an aim.

The presence of the excess charge in a shower may emit Cherenkov and bremsstrahlung radiation in a uniform medium. But the bremsstrahlung radiation is suppressed by LPM effect [10] and dielectric material effect [11] in the radio wave range. LPM effect is caused by that the coherent formation zone extends to the longitudinal direction due to the small longitudinal momentum transfer by the uncertainty principle. In the process of Coulomb multiple scattering of electrons in the coherent formation zone, radio emission gets destructive interference effect. For 2.5 MeV electrons, emission of radio wave under the frequency ~800 GHz is suppressed. Stronger suppression in the emission frequency comes from the dielectric material effect. Forward Compton scattering amplitude changes in phase giving destructive interference in the radio emission. For 2.5 MeV electrons, emission of photons under the energy ~150 eV is suppressed. Therefore practically only Cherenkov radiation effect should be considered in a uniform medium.

Wavelength λ of radio wave are compared at 1 GHz (λ = 0.3 m) and visible light at 1 PHz (λ = 0.3 μm) or 1×10^{15} Hz

$$\frac{\lambda(1\,\mathrm{GHz})}{\lambda(1\,\mathrm{PHz})} = 10^{6}. \tag{1}$$

Emission power of Cherenkov radiation is expressed by Frank-Tamm formula when charge z*e* travelling a path-length l with the velocity of $c\beta$ in a medium of refractive index n

$$\frac{dW}{d\nu} = (2\pi h\alpha / c)z^{2}\nu[1 - \frac{1}{(\beta n)^{2}}]l \tag{2}$$

Radiation power W at the frequency ν of 1 GHz and 1 PHz with the photon energies of 4.1×10^{-6} eV and 4.1 eV, respectively, are compared

$$\frac{\mathrm{W}(1\,\mathrm{GHz})}{\mathrm{W}(1\,\mathrm{PHz})} = 10^{-6}. \tag{3}$$

If we take into account the bandwidth, the power to be detected becomes hopelessly low ~10^{-12} to detect the radio wave. Visible wavelength is much shorter than the shower size, and then the radiation power is proportional to the total track length of the charged particles. The radiation power emitted by visible light $W_{visible}$ is expressed

$$\mathrm{W_{visible}} \sim \mathrm{N} < l >, \tag{4}$$

where N is the number of whole charged particles, $N(e^-)+N(e^+)$ with the average track length of $< l >$. The notations $N(e^-)$ and $N(e^+)$ are the numbers of electrons and positrons in the shower, respectively. On the contrary if the wavelength is larger than the shower size enough, radiated wave from each excess-negative charged track becomes constructively coherent with the same phase. Then the radiation power increases with the assistance of the coherent effect to a detectable level and is proportional to the average track length of charged particles times the square of negative excess charges $\Delta q \bullet N$, which is $N(e^-)-N(e^+)$. The radiation power for the radio wave, $W_{radiowave}$ is given

$$\mathrm{W_{radiowave}} \sim (\Delta \mathrm{q} \bullet \mathrm{N})^{2} < l >, \tag{5}$$

where Δq is a ratio of negative excess charges to the whole charges. $W_{radiowave}$ is amplified by a factor of $\Delta q^2 \bullet N$ compared with $W_{visible}$. The factor is the negative excess charges times Δq, which is described

$$\Delta q = \frac{\mathrm{N(e^-) - N(e^+)}}{\mathrm{N(e^-) + N(e^+)}}. \tag{6}$$

The possibility of using ice as the medium of the neutrino detector to propagate the radio wave is considered [12]. The excess electrons of the electromagnetic shower and coherent Cherenkov radiation by them are studied in detail in the case of ice [13]. The radiation power was calculated without absorption in the ice

$$W \sim 5\times10^{-14}[\frac{\mathrm{E}}{1\,\mathrm{TeV}}]^2[\frac{\nu_{\max}}{1\,\mathrm{GHz}}]^2 \text{ erg} \sim 5\times10^{-15} \text{ J}. \tag{7}$$

Where we assume E = 1 PeV, ν_{max} = 1 GHz.

They estimated the threshold energy E_{th} for the electromagnetic shower as a function of distance to the observation. At the distance of R (km), the detectable threshold energy with a receiver noise of 300° K thermal equivalent with the bandwidth of 1 GHz becomes,

$$\mathrm{R\ (km)} \sim \frac{\mathrm{E_{th}\ (PeV)}}{4}. \tag{8}$$

The excess electrons (Δq) are reported to be 15 % of the total track-length of particles in ice [13]. They are caused by the interaction of photons, positrons and electrons in the shower with the atomic electrons in the medium and generated by the Compton (~60 %) and Bhabha scattering (~30 %), and positron annihilation in flight (~10%). On the contrary, Moller scattering decreases the excess charge (~ -5 %) due to the energy loss by the collision. Radio Ice Cherenkov Experiment (RICE) in Antarctic ice is being executed successfully and gave a neutrino flux limit [14]. Recently, Radio-frequency measurements of coherent transition and Cherenkov radiation is done using a 15.2 MeV pulsed electron beam at the Argonne Wakefield accelerator. They detected coherent radiation, which is attributed both to transition and possibly Cherenkov radiation [15]. The coherent radiation was confirmed that the radiation strength was proportional to the square of the number of electrons in a single pulse.

Comparison with optical Cherenkov radiation

Detection of optical Chrenkov radiation is the well-established method using water (IMB, S-K, DUMAND, NESTOR, Lake Baikal, ANTARES, etc.) and ice (AMANDA, ICECUBE) [14] as the radiator. They could detect Cherenkov radiation emitted by high-energy charged particles faster than the velocity of light in the medium. The detection of the light is done well-developed photo-multiplier tubes, which could detect even one photoelectron converted at the photo cathode from an optical photon. The conversion efficiency (quantum efficiency) is over 20 % in the optical wavelength region. Therefore only one charged particles passing in the detection region could be measured easily. Moreover muons could be detected even if a muon passed the detector region which was produced in muon-neutrino charged-current interaction at a long way off. As a result it could provide a large mass of neutrino reaction volume although the initial energy is not determined so definitely due to being insensitive to the energy loss between the interaction point to the detector.

Meanwhile radio Cherenkov detection method could not detect single muon, and could not utilize the long range of high-energy muons. But it utilizes special characters that the radiation power is roughly proportional to the square of the shower energy due to the coherence effect among radio Cherenkov radiation from the excess electrons in the shower. And the attenuation length of radio wave is long in the medium. Consequently, the radio sensors could be set sparsely in a huge medium. The electron and the tau neutrinos could be detected with the information of the energy and the incident direction utilizing the specific Cherenkov radiation pattern in the same way as the optical Cherenkov detectors. Although for a muon generated by a charged-current interaction of a muon neutrino, it could not be registered after it escaped from the shower generated at the interaction.

Consideration on the medium density

We compare density, radiation length, refractive index, Chrenkov angle and Cherenkov threshold kinetic energy of electrons for air, ice and rock salt in Table 1.

TABLE 1. Comparison between air, ice and rock salt in density, radiation length X_0, refractive index, Chrenkov angle θ_c and Cherenkov threshold kinetic energy for electrons T_{th}.

	Density (g/cm^3)	**X_0 (cm)**	**Refractive Index**	**θ_c (deg)**	**T_{th} (keV)**
Air (STP)	0.0012	30420	1.000293	1.387	2060407
Ice	0.924	39	1.78	55.8	107
Rock salt	2.22	10	2.43	65.7	50

The density of air is 1/833 times less than rock salt and the radiation length is 3042 times larger than that even on the earth surface. Then the shower length and the diameter are much larger than ice and rock salt. The detection is not easy for such an extended air shower. In addition Cherenkov or fluorescent light detection in air shower depend on weather condition severely as well as the Sunlight, the Moonlight, lightning and artificial light. Direct particle detection of the UHE shower by the particle detector set on the surface is not affected by such the conditions but the detection of horizontal air showers is difficult. Underground detectors neither depend on the weather nor the Sunlight and the Moonlight. In principle they could furnish the same detection ability for all the time and the directions of the neutrino incidence.

In comparison with ice, rock salt has 2.4 times higher density, shorter radiation length (~1/4) and 1.4 times larger refractive index. Then the high-energy particle shower size is small owing to the high density. For electrons, the Cherenkov angle is large and the threshold energy is small due to the high refractive index. Consequently, rock salt is adequate medium to get larger Cherenkov radiation power. The frequency at the maximum electric field strength at θ_c is ~2 GHz without the absorption in ice [13]. Whereas it would increase up to ~5.6 GHz taking into account the short radiation length and the wavelength contraction due to the higher refractive index.

When a UHE proton hits the atmosphere, it could not put the large energy deposit underground in a narrow region. Radio-wave neutrino detector could sense only from many tracks of excess electrons inside the concentrated region with the help of strengthening by the coherence effect. For high sensitivity detector e.g. optical Cherenkov detectors, which could detect single muons, a great number of downward muons become large backgrounds. On the contrary the radio Cherenkov detector is immune from the muons. Therefore, practically only UHE neutrinos could induce the electric field on the radio antennas underground. However it could be a shortcoming when we intend to detect abundant lower-energy neutrinos in high statistics.

Normally, rock salt is covered by thick soil, which absorbs electromagnetic wave completely. Then SND is background free from natural or artificial radio wave coming from the surface on the earth. As a result background is only blackbody radiation corresponding to the temperature of the surrounding rocks. As the remaining potential background, radiation may come from a seismic movement of the surrounding rocks, which may generate radio wave due to the piezoelectric effect by the stress in the rocks. If such a radiation could be detected, the observation contributes to the seismology.

Appearance of tau neutrino due to oscillation

Detection of high-energy cosmic tau neutrinos [16] could be achieved by making use of the characteristic double shower events [17] in the detector medium. The two showers are connected by a μ like track. The size of the second bang is on the average a factor of two larger than the first bang. Electron neutrinos produce a single bang at these energies whereas the muon neutrinos typically produce a single shower along with a zipping μ -like track. Based on these rather distinct event topologies, cosmic neutrino flavor may be conceivable. We assume the standard ratio of the intrinsic cosmic neutrino flux being $F(\nu_e)$: $F(\nu_\mu)$: $F(\nu_\tau) \cong 1:2:0$ at the production. With the constraints of the solar and atmospheric neutrino and the reactor data, we obtain that the ratio of the cosmic high-energy neutrino fluxes in the far distance is 1:1:1, irrespective of which solar solution is chosen.

Possible experimental sites of rock salt mine for SND

We searched a medium which has long attenuation length in a Science chronological table [18]. Then we found that rock salt has one of the lowest $\tan\delta$ of 5-1×10^{-4} in the wide range in the radio frequency of 1 kHz - 10 GHz with the relative real permittivity of 5.9. The loss angle $\tan\delta$ is the ratio of the imaginary divided by the real part in the complex permittivity. The imaginary part presents the absorption in the material. Therefore smaller $\tan\delta$ means longer absorption length. But if water is present in the rock salt, the transparency reduces much. Another idea come from a finding that rock salt is free from water permeation described in a topography dictionary [19]. On the salt dome, petroleum or natural gas are likely to deposit. They are covered with soil, which prevents radio wave to penetrate from the surface. Unfortunately there is no rock salt in Japan. In that era, Japan had no chance to form rock salt since it was under the ocean.

Due to the characters of no water permeation and the long time stability, they are used to maintain radiation wastes, e.g. Asse and Gorleben salt mines in Germany, and WIPP (Waste Isolation Pilot Plant) at USA. Some laboratory measurements of RF complex permittivity had been made on a variety of rocks encountered in mining, tunneling, and engineering works. An RF impedance bridge and a parallel-plate capacitance test cell were employed at frequencies of 1,5, 25, and 100 MHz [20]. In their measurement rock salt was the most transparent for the radio wave.

Rock salt had beam made in old days, around 250 millions yeas ago when a huge ocean was situated in a hot, dry desert climate. As the water in a closed region evaporated, dissolved substances were left behind. Marine sediments later buried these deposits, but since halite is plastic and less dense than the materials that make up the overlying sediments, the salt beds often punched up through the sediments to create dome-like structures. Additional sediments now mostly bury these. Salt consists of the two basic elements, sodium and chlorine, and forms colorless, cube-like crystals. Various additional elements such as iron, potassium, magnesium or calcium, discolor the slat and also alter its taste; magnesium produces a bitter taste and potassium a soapy one. There are many rock salt basins in the world [21].

We had visited five rock salt mines. Among them, at Austria, we went to see Durrenberg salt mine at Hallein near Saltzburg and Altaussee salt mine at Salzkammergut, July 1999. Durrenberg salt mine already closed mining 10 years ago and active only for sight seeing. The Altaussee is still active to produce salt by the borehole brine method. The entrance of the salt mine is located at the mountainside going into horizontally. The temperature inside the tunnel was around 5°C. It is said to be the largest and the cleanest among European Alps rock salt mines. The surfaces of the tunnels got wet and there were lakes underground. Tourists could ride on a boat in the lake. As far as the view from the sightseeing course, it seemed that it was not adequate for the radio wave passage inside the rock salt since the water penetrated rock salt crevices might absorb radio wave much.

We visited Asse research mine on August 1999 and March 2000, which is located near Braunschweig between Hanover and Berlin, Germany. The Asse is a range of hills of approximately 8 km length in the northern Harzforeland. In the course of geological time, the Zechstein salt deposited on the ocean floor migrated into the core of the Asse structure. The mine is used as an underground laboratory to be a service facility of the GSF-National Research Center for Environment and Health. Most of the tunnels would be used to store radiation wastes. We could go down driving a car through a spiral section (average gallery incline 10 %) between 490 m and 930 m levels as well as by a facility of elevators in shafts. The Asse salt mine consists of vertical area between 490 and 850m depth, divided into 16 levels. At the present, the lower area of the salt structure is being mined to the planned level of 930 m. The horizontal tunnels make a lattice extended nearly 750 m at each levels. Air was sent inside to cool down the temperature. The humidity was low. Near the bottom there was a low background radiation laboratory operated by PTB (the Physikalisch-

Technische Bundesanstalt in Braunschweig, Germany). In the rock salt environment, natural radiation background from uranium and thorium is lower than inside of normal rocks. In Asse mine, a group from Hanover studied the salt bodies used as the repositories for nuclear waste using a 50 MHz ground-penetrating radar. They had succeeded to find positions and shapes of cavities and other kind of rocks other than the rock salt in tomographically [22].

The Hockley salt mine is near Houston, Texas. The salt mining is executed for commercial use. There is an underground "The Hockley Seismic Station" operated by the Institute for Geophysics, University of Texas and is a cooperative project between the University of Texas, IRIS, USNSN, and the United Salt Corporation. The Hockley seismometer is located in an excavated chamber within an active salt mine owned by United Salt Corporation. The chamber lies approximately 470 meters below the surface within a large salt dome. Locating the instrument within a salt dome reduces the noise from human activity that generally affects instruments on the surface. The air was dry and the temperature was rather high. Tunnels are developed as a lattice nearly 1 km at the underground level. The salt dome size seems enough for SND.

The Waste Isolation Pilot Plant (WIPP) is the first underground repository licensed to safely and permanently disposes of transuranic radioactive waste left from the research etc. in USA. After more than 20 years of scientific study, public input, and regulatory struggles, WIPP began operations on March, 1999. It is located in the remote Chihuahuan Desert of Southeastern New Mexico; project facilities include disposal rooms mined 540 m underground in a 500m thick salt formation that has been stable for more than 200 million years. The tunnels are excavated nearly 1 km in a lattice style. Over the next 35 years, WIPP is expected to receive shipments. The temperature of the rock salt is 24° C and the air is dry. One of the cavities is planned to use underground experiments such as dark matter search etc. The rock salt extends horizontally in the wide range around WIPP although the salt deposit is not so deep. There is enough land of the governmental property to construct SND near WIPP.

Measurement of microwave absorption length in the laboratory and the noise measurement of a radiometer

We have measured complex permittivities of rock salt samples, shown in Fig. 1.

(a) (b) (c)

FIGURE 1. Photos of rock salt samples from Hallstadt salt mine: a) 200mm × 200mm × 30mm, b) 200mm × 200mm × 11mm, Austria, and Asse salt mine: c) 200mm × 200mm × 99mm], Germany.

The samples from the Hallstadt salt mine are colored in brown and have a striped pattern. On the contrary, the sample from Asse salt mine is white and has no striped pattern. It seems the rock salt consists of small crystals.

A free space measurement method was employed which had been used in a non-destructive manner for the assessment of microwave materials [23]. The principle of the method is illustrated in Fig. 2. The vector network analyzer HP85107A measures the strength and the phase of the scattering wave with and without a metal-plate reflector on the sample. The feature of the method is the ability to subtract the effect from the background wave scattered from the wall and the floor, etc. other than the area of the sample covered with the metal-plate reflector, namely measuring area. By displacing the position of the metal-plate reflector on the specimen to be tested, the incident wave and the scattered wave from the measuring area were determined without the influence of extraneous waves such as the direct coupling between the transmitting and the receiving antennas and scattered waves from the background objects. The behavior of the metal-plate reflector is similar to that of an optical shutter in optics. The photograph of the equipment is shown in Fig. 3.

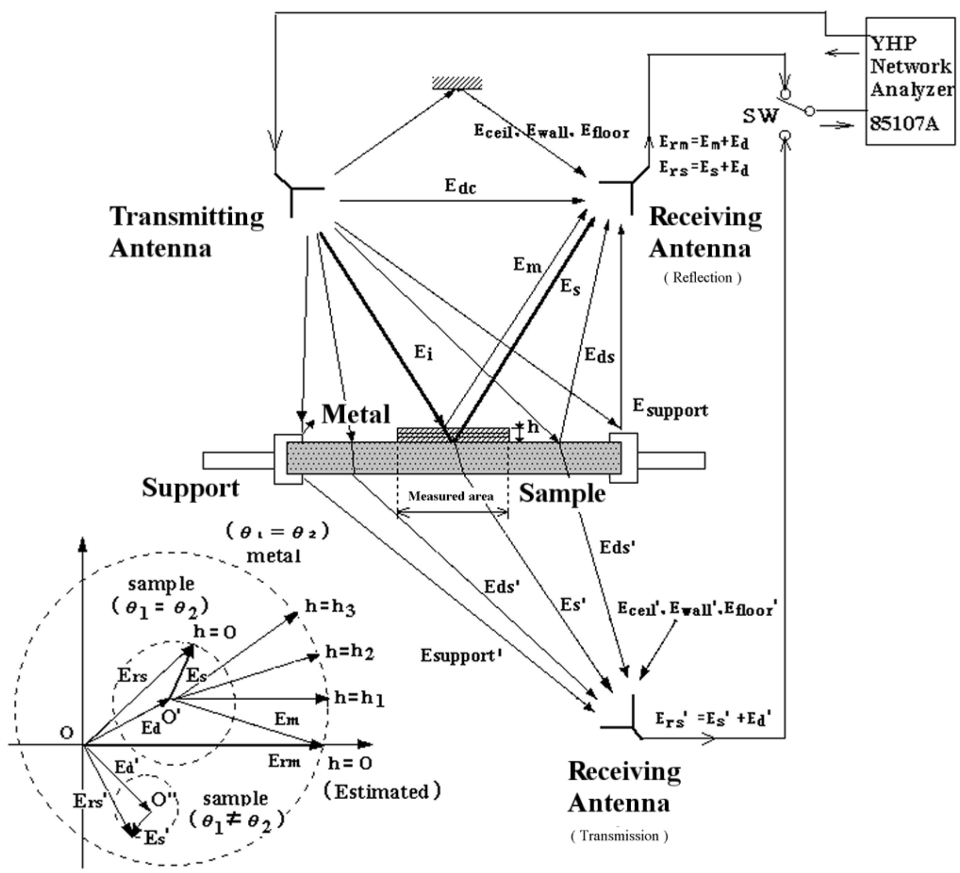

FIGURE 2. Principle of the measurement is illustrated with various wave components. A vector diagram of the received signals is shown with and without the metal-plate reflector on the sample.

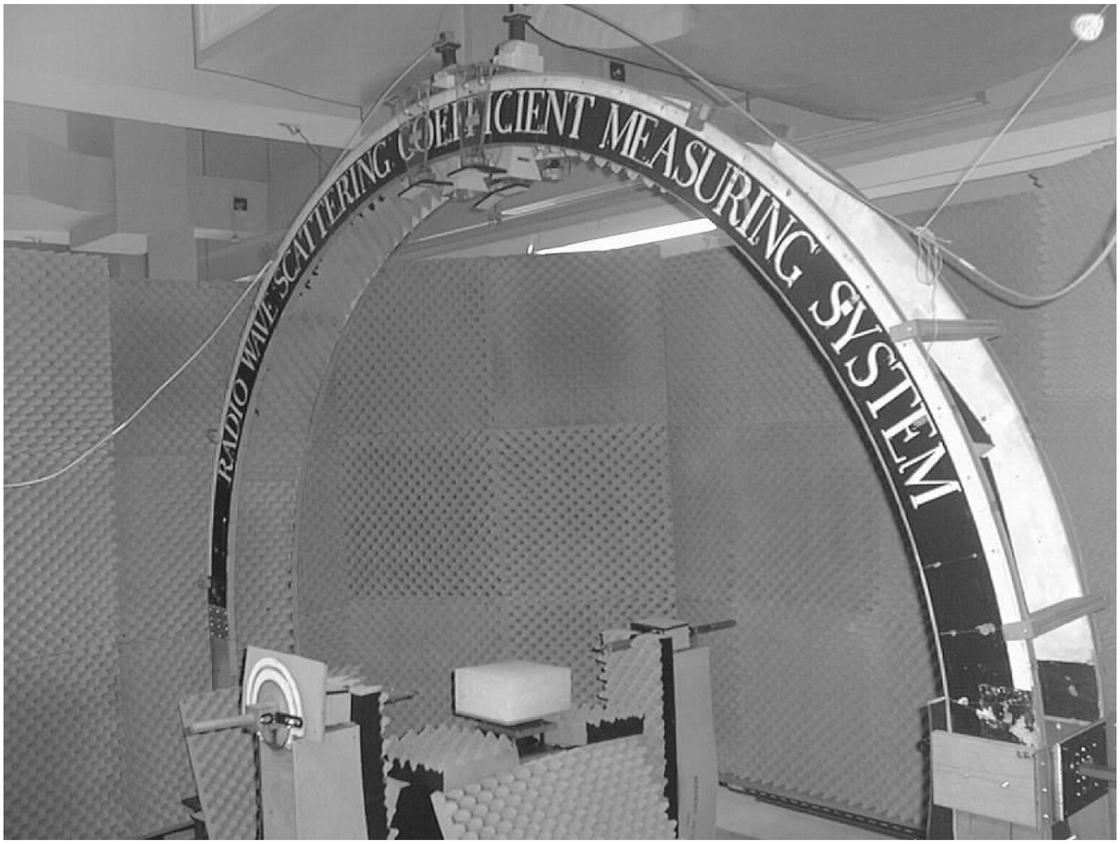

FIGURE 3. Photograph of the measuring apparatus in the X-band region with the sample from Asse salt mine. The transmitting and receiving horn antennas are so set at the upward on the arch that both the incident and scattering angles become 5°. The diameter of the arch is 2.6 m.

In Fig. 2 the illustration shows the measurement with the metal-plate reflector where three metal plates are piled up on the sample to adjust the height of the metal plate surface. The receiving antenna is set at the reflection configuration. Just for instance, the configuration of transmission measurement is also given. The notations $\mathbf{E_m}$, $\mathbf{E_s}$ and $\mathbf{E_d}$ mean scattered signals from the metal plate, the measuring area of the sample and the background objects, respectively. The received signals of $\mathbf{E_{rm}}$ and $\mathbf{E_{rs}}$ are the scattered signals from the metal-plate reflector $\mathbf{E_m}$ with the background $\mathbf{E_d}$, and the sample within the measuring area $\mathbf{E_s}$ with the background $\mathbf{E_d}$, respectively. Changing the height of the metal-plate reflector gives a small difference in the path length between the antennas and the metal-plate reflector, which alters the phase of the scattering wave from the metal-plate reflector only. In the vector diagram the horizontal and the vertical axes express the real and the imaginary coordinates, respectively. The large and the small circles show the cases with and without the metal-plate reflector, respectively. The heights of the metal-plate reflector in the different path lengths are expressed as h = 0, h_1, h_2 and h_3 on the large circle for $\boldsymbol{E_m}$. At the small circle, $\mathbf{E_s}$ is shown at h = 0 without the metal-plate reflector. We could subtract the background effect deducting $\mathbf{E_d}$.

As shown in Fig. 3, the sample was set horizontally on a metal table, which could be lifted up and down to adjust the height of the surface of the metal-plate reflector or the sample. The microwave was irradiated downward with the incident angle of 5° to a sample by a horn antenna having an aperture of 97 mm × 68mm at 8.0-10.0 GHz. The reflected radio wave was detected by another horn antenna of the same aperture with the same angle of 5°. The distance from the horn antennas to the sample was 1.3 m. The distance from the antennas was adjusted to keep the same in the two cases of with and without the metal-plate reflector of 200 mm × 200 mm × 3 mm on the sample.

The measurement was done at 7 heights of the sample or the metal-plate reflector being separated in 2mm, which correspond to $\lambda/8$ changes in the path lengths in the air. The measured complex values of 7 received signals are plotted in Fig. 4 with (solid line) and without (dashed line) metal-plate reflector.

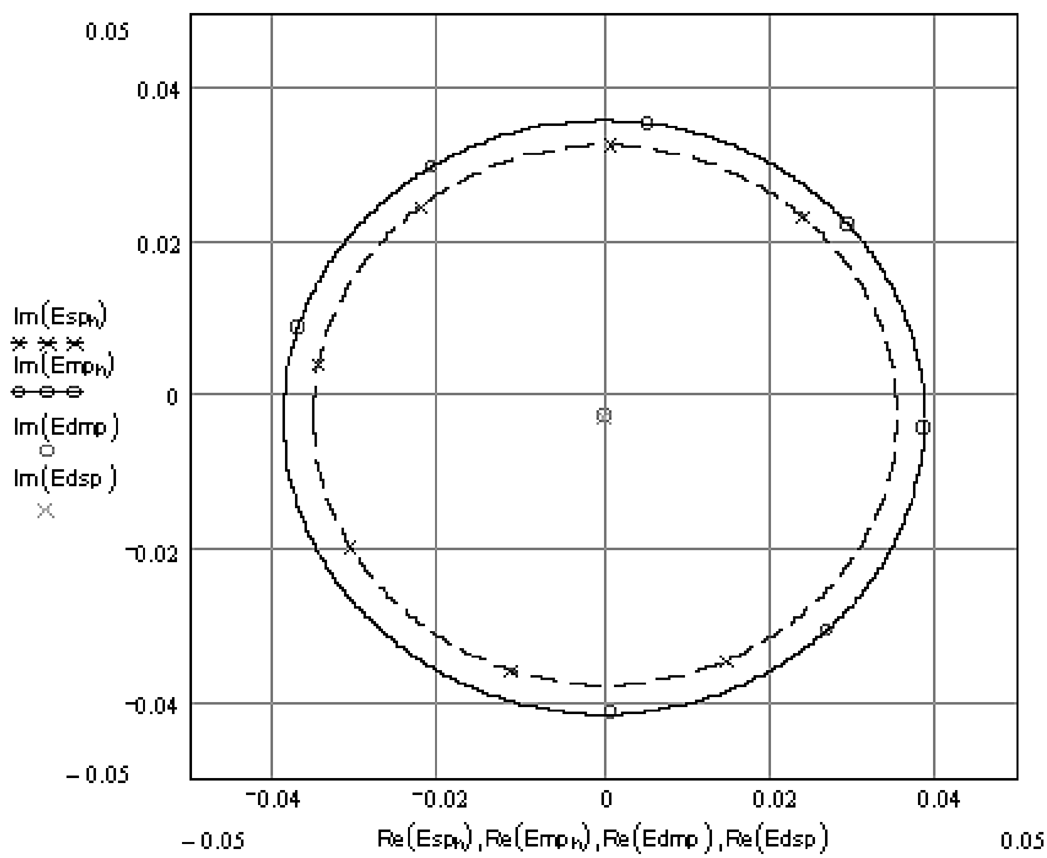

FIGURE 4. The measurement was done at each position of the sample being separated in 2 mm, which corresponds to $\lambda/8$ changes in phase. The measured complex values of received signal are plotted in each position with (solid line) and without (dotted line) metal plate. The figure is in parallel polarization with the scattering plane. The 7 measured points in each circle with (circle) and without (cross) the metal-plate reflector are fitted, and the centers are found to be coincident.

Figure 4 shows the vectors of $\mathbf{E}_{\mathbf{rm}}$ from the origin to the large circle and $\mathbf{E}_{\mathbf{rs}}$ to the small circle in parallel polarization with the scattering plane, respectively. The notations are the same at Fig. 2. The centers of the two circles coincide so precisely that the background signal E_d is the same in the two cases. Also the centers are so close to the origin that the background signal $\mathbf{E_d}$ is small. Naively, in case of a single reflection at the bottom surface of the sample, the angle and the radius differences in the complex plane correspond to real and imaginary permittivity, respectively. In more precise analysis, we take into account the multiple paths between the upper and the lower surfaces inside the sample. The complex permitivity was deduced from the ratio (scattering coefficient) of the complex measurements of the electric fields as $\mathbf{E_{rs}}$ /$\mathbf{E_{rm}}$. The measured real part of the complex permittivities are tabulated in Table 2 as the linear polarization of parallel R_p and perpendicular R_s with the scattering plane. The values are well consistent each other and with the value of 5.9 tabulated in the handbook [18]. While the measurement accuracy is not enough at the present in the imaginary part of the permittivity. The imaginary parts have different values in the samples a) and b). Both were cut from the same block. For the time being we could say the imaginary part of the permittivity is between 6×10^{-4} and 6×10^{-3}, namely tanδ is between 1×10^{-4} and 1×10^{-3} at 10 GHz.

TABLE 2. Real part of complex permittivities in rock salts

Thickness / Polarization	R_p	R_s
Hall Statt 11.1mm	5.9	6.0
Hall Statt 30.1mm	5.9	6.0
Asse Mine 99.0mm	5.9	5.9

We could calculate the absorption coefficient α:

$$\alpha = \frac{\omega}{c}\sqrt{\varepsilon'}\frac{\tan\delta}{2}, \tag{9}$$

where the notations are following, complex permittivity ε:

$$\varepsilon = \varepsilon' - j\varepsilon'' = \varepsilon'(1 - j\tan\delta), \tag{10}$$

loss angle in the permittivity $tan\delta$:

$$\tan\delta = \frac{\varepsilon''}{\varepsilon'}, \tag{11}$$

complex refractive index $\boldsymbol{n}$:

$$n = \sqrt{\varepsilon} = \sqrt{\varepsilon'}\sqrt{1 - j\tan\delta}. \tag{12}$$

When the value of $tan\delta$ is 1×10^{-4} or $1x10^{-3}$, α becomes 0.025/m or 0.25/m, respectively, at 10 GHz. As the result we get the absorption lengths $1/\alpha$ as 40 m or 4 m. Assuming $tan\delta$ is constant with respect to the frequency, the absorption length comes 400m or 40 m at 1 GHz.

We are planning to measure natural rock salt samples by a perturbed cavity resonator method at 9.4GHz [24]. The drawing of the cavity is shown in Fig. 5. The photograph of the apparatus is presented in Fig. 6.

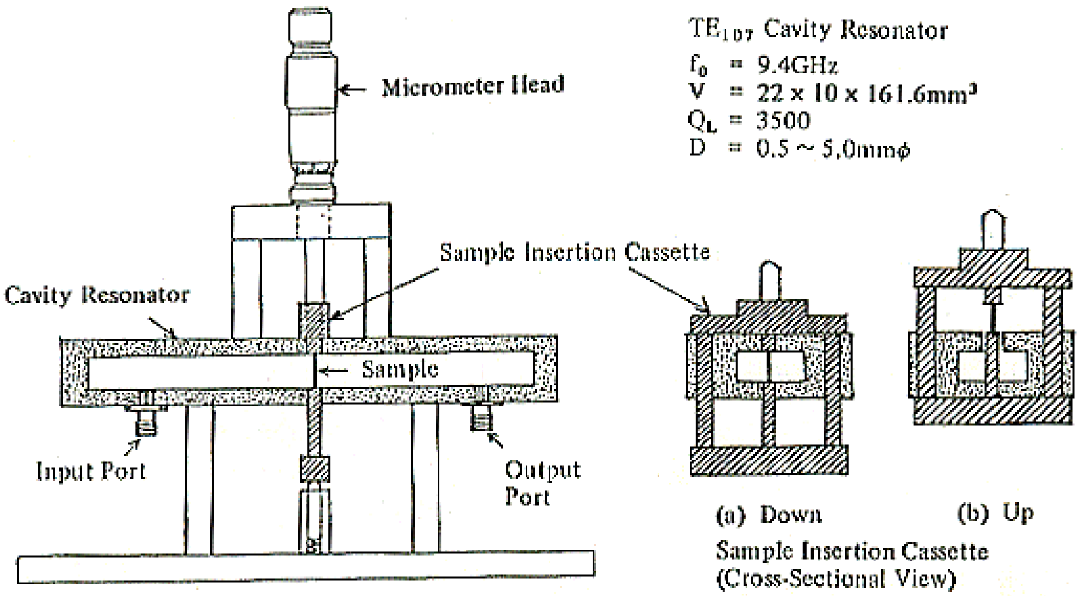

FIGURE 5. Illustration of the perturbed cavity resonator.

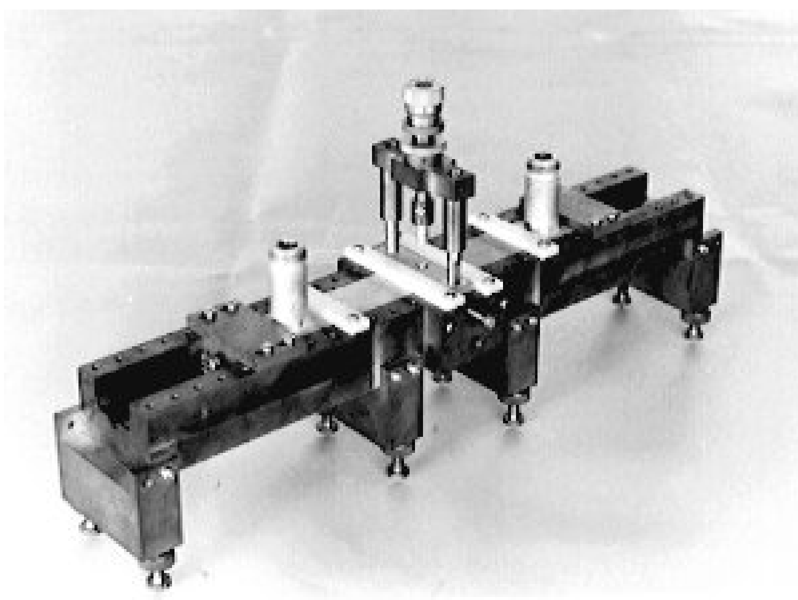

FIGURE 6. Photograph of the perturbed cavity resonator.

Using the apparatus the complex permittivity ε could be measured. The principle of the measurement in the real ε' and the imaginary ε'' of the complex permittivity is the changes in the center frequency and the width of the resonance, respectively, with and without insertion of the sample in the cavity. The thin sample is needed to the small perturbation for the resonance behavior. The imaginary ε'' depends on the change of the Q factor (the ratio of the resonance frequency to the resonance width). In order to get the value, we should take into the volume ratio of the sample to the cavity. We could cleave a synthetic rock salt sample to the size of 1 mm $\times$ 1 mm $\times$ 10.2 mm. By that method we have got the result of the synthetic rock salt as $\varepsilon = 5.8 - j3.5 \times 10^{-4}$ or $tan\delta = 0.6 \times 10^{-4}$ which is a little bit lower than the value tabulated in ref. [18]. While we have not succeeded to cleave the natural samples to the size.

We have tested a noise level of a radiometer system. The main part of the radiometer is a modified TV Broadcasting Satellite (BS) receiver, which is an amplifier-converter module with the center frequency of 10.6 GHz. The system is composed of the horn antenna having the aperture of 97 mm $\times$ 68mm, the amplifier-converter module, a 30 dB amplifier, a rectifier and a time chart recorder or an oscilloscope. The amplifier-converter module consists of a signal conversion part from the wave guide of the horn antenna to a coaxial style, 3-stage low noise HEMT amplifiers with filter at the center frequency of 10.6 GHz (band-width of 200 MHz), and frequency converter to which the local oscillator signal of 9.6 GHz is introduced from outside. After the conversion part, the signal is amplified with another 3-stage amplifier in the module. The horn antenna is directed vertical to the sky having ~30° K noise or covered with a ~300° K thermal noise material. The comparison of the signal strengths, we could get the noise level of the amplifier-converter module as low as 150° K. The noise level is well below the rock salt temperature. Due to the results we could afford to get a lot of the receivers with low cost which is the modified BS receiver used by popular TV audience.

SND is envisaged as shown in Fig. 7. Radio wave sensors of 216 are arrayed regularly in 200m repetitions inside a 1km $\times$ 1km $\times$ 1km rock salt. The attenuation length becomes longer when we use the lower frequency to be detected. However the detection threshold energy of UHE neutrinos reduces at the lower frequency. The optimization should be done to select the frequency. If the attenuation length is 400 m, the sensor separation distance less than 200 m is needed to detect the Cherenkov ring shape as well as the energy. Six radio sensors are hung on a string. The string is lowered in a well with the depth over 1km. At the total 36 wells should be bored.

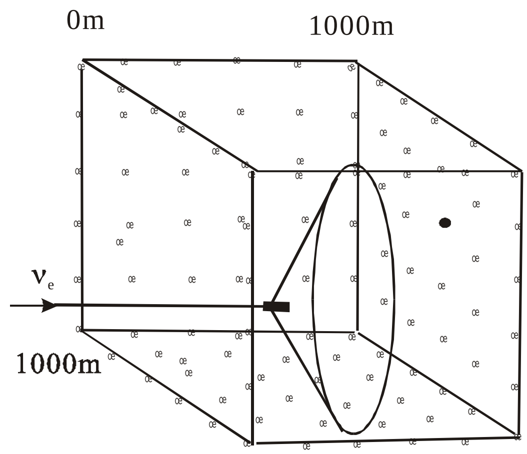

FIGURE 7. Salt Neutrino Detector underground. Excess electrons in the shower at the UHE neutrino interaction generate a coherent Cherenkov radiation with the emission angle of 66°.

Summary

Rock salt is studied as a radio wave transmission medium in the UHE cosmic neutrino detector. The radio wave would be generated by Askar'yan effect (coherent Chrenkov radiation from negative excess charges in the electromagnetic shower) in the UHE neutrino interaction in the rock salt. Some rock salt mines were investigated whether it has a possibility as a SND site or not. We found that there were potential sites to construct SND. The samples of the rock salts were gathered to measure the absorption length. As a tentative result, the absorption length of the radio wave was obtained to be between 400m and 40 m at 1 GHz.

The preliminary results of the radio wave absorption length in the rock salt show that it has a chance to be used as the medium of UHE neutrino detector when we select a rock salt mine in good transparency. We need to measure in the lower frequency and more samples as well as in the perturbed cavity resonator method to deduce the concrete conclusion. Before the site is decided, it is important to measure the absorption length in *situ*. There may be defects and impurities as well as intrusions by rocks other than rock salt. For that research it is useful to employ the ground penetrating radar, which is a well-explored technique.

Further we studied a radiometer modified from TV BS receiver, which showed the noise level of 150° K. The level is low enough to implement SND. It is advantageous if we could use the low cost receivers. Large number of antennas is needed in the configuration of the antennas spacing less than 200 m in a 1km × 1km × 1km rock salt. The attenuation in the rock salt and the radiation pattern of the coherent Cherenkov radiation require the repetition of the antennas. The radio frequency should be decided taking into account the detection energy threshold of UHE neutrinos and the attenuation length. In addition it is indispensable to study the basic process on the coherent Cherenkov radiation due to a pulsed electron beam supplied by an accelerator. By the research we could calibrate the energy of the initial electromagnetic shower by the detected radiation power, which depends on how much coherency is realized.

ACKNOWLEDGMENTS

This work was supported partly by Funds for Special Research Project at Tokyo Metropolitan University, Fiscal Year 1999. We should appreciate Profs. K. Minakata and T. Kikuchi (TMU) to support this project.

We express our gratitude to M.E. Ryouichi Ueno who discussed with and advised us about the microwave techniques. He was indispensable to carry out this study.

The research could not be possible without the assistances from and discussions with many persons because parts of the field researched were far from our specialized field. Here we express our appreciations to those who have interests and extended their favors on our research.

Prof. Tuneaki Daishido (Wasada University, Tokyo) instructed us about the low noise microwave detection and transferred us the amplifier-converter. M.E. Yoshinori Sanada (Kyoto Univ.) gave us the penetration rate of electromagnetic wave underground. Messrs. Akiharu Kitahara and Hisashi Itou (Tokyo Metropolitan Industrial Technology Research Institute) informed us low energy electron accelerators available. Messrs. Yuichi Chou and Teruhisa Hirashima (Denki Kogyo Co. Ltd.) provided us an opportunity to use a compact RF accelerator for electron beam irradiation.

The information and the samples of Austrian rock salt mines were got from Profs. Franz Mandl, Jimmy MacNaughton (Institute for High Energy Physics, Austria), Komarek (Wien University, Austria) and Dr. Doz.Weber (Ministry of Economy, Austria) and Mr. Masayuki Handa (Tobacco and Salt Museum, Tokyo).

Prof. Motoyuki Sato (Tohoku Univ.) introduced us ground-penetrating radars in a rock salt mine at Asse research mine. We are indebted for the call at the Asse mine and getting the sample to Dr. Dieter Eisenburger (Federal Institute for Geosciences and Natural Resources, BGR, Hanover, Germany), Dr. Stefan Neumaier and Mr. Eberhard Funk (Physikalisch-Technische Bundesansalt, Braunshweig, Germany). Messrs. Nobuteru Hitomi and Yoshiharu Kobayashi (Mechanical Engineering Center, KEK) cut us the rock salt samples.

We appreciate those who informed us about salt domes concerning to petroleum minings; Messrs. Shin-ichi Inoue (Abu Dhabi Oil Co., Ltd.), Hitoshi Takezaki (Japan Energy Development Co., Ltd.), Yoshihisa Tanaka, Taizo Uchimura, Toru Akutsu, Dr. Osamu Takano (Japan National Oil Corporation), and Mr. Greg Jones (Exxon, New Orleans, USA).

We are indebted to Prof. Yoshio Nakamura (Institute for Physical Geology, University of Tesax) and Mr. Marcelino Segura (United Salt Corporation, Hockley Plant) for visiting Hockley Salt Mine (United Salt Co., Houston, Texas, USA).

At the visiting of WIPP, We were taken care of by Prof. Shinjiro Mizutani (Nihon Fukushi Univ.), Dr. Hidekazu Yoshida (Nuclear Fuel Cycle Development Institute), and Dr. Erik. K. Webb (Sandia Institute, USA), Dr. Roger Nelson, Ms. Beth Bennington, and Mr. Norbert T. Rempe (Waste Isolation Pilot Plant, Carlsbad, New Mexico, Department of Energy, USA).

REFERENCES

1. Stecker, F. W., Done, C., Salamon, M. H., and Sommers, P., *Phys. Rev. Lett*. **66**, 2697-2700 (1991).
2. Barwick, S., Halzen, F., Lowder, D., Miller, T., Morse, Price, P.B. and Westphal, A., *J.Phys. G:Nucl. Part. Phys.* **18**, 225-247 (1992); Thomas K.Gaisser, Francis Halzen, Todor Stanev, *Phys. Reports* **258,** 173-236 **(**1995).
3. Takeda *et al*.., *Phys. Rev. Lett*. **81**, 1163-1166 (1998).
4. Greisen, K., *Phys. Rev. Lett*. **16,** 748 (1966); .Zatsepin, G.T., Kuz'min, V.A., *Zh. Eksp. Teor. Fiz*., *Pis' ma Red.* **4**, 114 (1966) [*Soviet Physics JETP Lett.* **4**, 78 (1966)].
5. Burdman, G., Halzen, F. and Gandhi, R., *Phys. Lett*. **B417**, 107-113 (1997);.Jain, P., Mckay, D.W., Panda, S., Ralston, J. P., *Phys. Lett*. **B484**, 267-274 (2000).
6. Gandhi, R., Quigg, C., Reno, M.H. and Sarcevic I., *Astroparticle Phys*. **5,** 81-110 (1996); *Phys. Rev*.**D58**, 093009: Sigl, G. *Phys. Rev*. **D57**, 3786-3789 (1998): Kwiecinski, J., Martin, A.D., Stasto, A.M., *Phys. Rev***.D59**, 093002 (1999); Horvat, R., *Phys. Lett*. **B480**, 135-139(2000).
7. Athar H., Presentation at the seminar of high-energy theory group, Oct. 2000, TMU.
8. Fukuda Y. *et al*., SuperK Collaboration, *Phys. Rev. Lett*. **81**, 1562(1998).
9. Askar'yan, G.A., *Zh. Eksp. Teor. Fiz*. **41**, 616-618 (1961) [*Soviet Physics JETP* **14**, 441 - 442 (1962)]; **48**, 988 - 990 (1965) [**21**, 658 - 659 (1965)].
10. Landau, L. D., Pomeranchuk, I. Ya., *Dokl. Akad. Nauk SSSR* **92**, 535 (1953); **92**, 735 (1953); Migdal, A.B., *Phys. Rev.*, **103**, 1811-1820 (1956); Klein, S., *Rev. Mod. Phys***. 71**, 1501-1538 (1999).
11. Ter-Mikaelian, M. L., *High-Energy Electromagnetic Processes in Condensed Media*, Interscience Tracts in Physics and Astronomy, Number 29, Wiley-Interscience, a Division of John Wiley & Sons, Inc., New York, (1972), ISBN 0-471-85190-6.
12. Markov, M.A. and I.M.Zheleznykh, and I.M.. *Nucl. Instrum. Methods.* **A248,** 242-251 (1986).
13. Halzen, F., Zas, E.,.Stanev, T, *Phys. Lett.* **B257,** 432-436 (1991); Zas, E., Halzen, F., Stanev, T., *Phys. Rev*. **D45,** 362-376 (1992); Alvarez-Muniz, J. and Zas, E. *Phys. Lett*.**B411,** 218-224 (1997); Frichter, J.M., Ralston, J.P. and .Mckay, D.W., *Phys. Rev*.**D53,** 1684-1698 (1996).
14. The most recent status of large high-energy neutrino detectors are shown in the presentation transparencies in 19th International Conference on Neutrino Physics and Astrophysics (Neutrino 2000), 2000, Sudbury, Canada at URL http://ALUMNI.LAURENTIAN.CA/www/physics/nu2000/.
15. Gorham, P., Saltzberg, D., Schoessow, Gai, P.W.,.Power, J. G., Konecny, Richard and Conde, M.E., *Phys. Rev*. **E62**, 8590-8605 (2000).
16. Halzen, F., Saltzberg, D. *Phys. Rev.Lett***., 81**, 4305-4308 (1998).
17. J.G. Lerarned, G. and Pakvasa, S., *Astropart. Phys*. **3**, 267(1995); Athar, H., Jezabek, M. and Yasuda, O., *Phys. Rev*. **D62**,103007 (2000); Athar, H., *hep-ph*/9912417, 1999; Athar, H., *Nucl. Phys*. **B(Proc. Suppl.)76,** 419 (1999); Athar, H., Parente, G. and Zas, E., *hep-ph*/0006123(2000).
18. *Chronological Scientific tables* (in Japanese) edited by National Astronomical Observatory of Japan, Maruzen Co. Ltd., Tokyo, (1998) pp.486.
19. *Topography dictionary* (in Japanese) edited by Machida, T., *et al*., Ninomiya Book Co. Ltd., Tokyo, (1981) pp.110.
20. Cook, J.C., *Geophysics*, **40**, 865-885 (1975).
21. Stanley J. L., *Handbook of World Salt Resources*, Plenum Press, New York, (1969); Michel T. H., *Salt Domes*, Gulf Publishing Company, Houston (1979).
22. Mundry, E., Thierbach, R., Sender, F and Weichart, H., *Proceedings of the Sixth International Symposium on Salt*, **Vol.I**, 585-599 (1983); Nickel, H., Sender, F., Thierbach, R. and Weichart, H., *Geophysical Prospecting* **31**, 131-148 (1983); Sato, M. and Thierbach, R. *IEEE Transactions on Geoscience and Remote Sensing*, **29**, 899-904 (1991); Eisenburger, D., *Proceedings of the 5th International Conference on Ground Penetrating Radar*, 647-659 (1994); Eisenburger, D., Gundelach, V., Sender, F., Thierbach, R., *Proceedings of the 6th International Conference on Ground Penetrating Radar*, 427-432 (1996).
23. Ueno, R. and Kamijo, Toshio, *IEICE Trans. Commun*. **E83B,** 1554-1562 (2000); Ueno, R. and Kamijo, T., *Memoirs of Graduate School of Engineering, Tokyo Metropolitan University*, 5743-5752 (1999).
24. Ueno, R. and Kamijo, T., *Memoirs of Faculty of Tech., Tokyo Metropolitan University*, 3923-3933 (1989).